Human Reproduction, Vol.27, No.S1 pp. i22–i49, 2012
doi:10.1093/humrep/des205

human reproduction

CHAPTER TWO

The zygote

Loredana Papale, Agnese Fiorentino, Markus Montag, and Giovanna Tomasi

Contents

Introduction

A series of dynamic and complex events are triggered following sperm–oocyte interaction that sequentially leads to fertilization and the formation of a zygote. These events include sperm penetration, sperm–oocyte fusion and oocyte activation, male and female pronucleus (PN) development and gradual migration of the pronuclei (PNs) to a central position in the oocyte.

Induced by the sperm penetration and subsequent calcium oscillations, the fertilized oocyte undergoes maternal-to-zygotic transition as a result of major changes in the molecular signals that control the arrest of meiotic development at the metaphase II stage of the second meiotic division (Ajduk *et al.*, 2011). In humans, the sperm centriole has the leading role in organizing the microtubules, which direct the migration of PNs and their rotation within the cytoplasm. In this way, PNs position their axis toward the second polar body and achieve a proper orientation at syngamy by controlling the plane of the first mitotic division. During PN formation, nuclear precursor bodies (NPBs) become evident and start to migrate and merge into nucleoli in a time-dependent manner. The NPBs do not form a functionally active nucleolus at the zygote stage; however, they can be used as an indirect measure of the location and the grade of condensation of DNA within the PNs. Nucleoli are the sites of synthesis of pre-rRNA and its availability is extremely important since newly synthesized rRNA is necessary for the translational processes when the embryonic genome becomes active (Gianaroli *et al.*, 2003). Asynchrony in the timing of any of the events associated with fertilization could compromise embryo development.

Once PNs are aligned onto a polar axis, parental chromosomes then separate in preparation for mitosis. The human zygote's mitotic potential is paternally inherited with the spermatozoon delivering the centrosome (Palermo *et al.*, 1994; Sathananthan *et al.*, 1996).

A zygote's morphological characteristics are accepted to be an inherent indicator of both gamete quality and subsequent embryo implantation potential (Alpha Scientists in Reproductive medicine and ESHRE Special Interest Group of Embryology, 2011). Many studies have underlined the predictive value of zygote morphological assessment through correlations with chromosome constitution and the incidence of zygotic arrest (Gianaroli *et al.*, 2003; Balaban *et al.*, 2004; Edirisinghe *et al.*, 2005; Zamora *et al.*, 2011). Recent strategies in embryo selection include sequential morphology assessment where PN scoring has been shown to play an important role as an indicator of gamete constitution as well as a prognostic tool for embryo competence. Scoring of PNs has also proved to be useful in countries where restrictive legislation mandates selection at the zygote stage for embryo transfer and consecutive elimination or cryopreservation of sibling zygotes (Senn *et al.*, 2006; Zollner *et al.*, 2005).

Although numerous studies have associated positive clinical results with the implementation of PN scoring, other reports have questioned the predictive value of PN scoring systems and see no benefits or improvement in the outcome (Nicoli *et al.*, 2010; Weitzman *et al.*, 2010). The Istanbul consensus workshop comprised a worldwide panel of experts who just recently evaluated the current practice of oocyte to embryo scoring and established common criteria for assessment (Alpha Scientists in Reproductive Medicine and ESHRE Special Interest Group of Embryology, 2011). Fertilization check is to be

performed at 17 ± 1 h post-insemination which may establish uniformity in the future and eliminate the variability in PN scoring regimens that have confounded comparative analyses. It must be noted, however, that the processes associated with fertilization by conventional insemination lags 1 h behind fertilization using ICSI (Nagy *et al*., 1998). A more complete elucidation of events during the zygote stage, however, can be expected with the application of continuous monitoring through the introduction of time-lapse imaging instead of the traditional isolated observations using light microscopy (Montag *et al*., 2011).

Normal fertilization is assessed by the presence of two centrally positioned, juxtaposed PNs with clearly defined membranes and two polar bodies. If an abnormal PN number is observed whether it be 1, or 3 or more, PNs, a low viable pregnancy is to be expected thus the transfer of these zygotes is to be avoided (Reichman *et al*., 2010). Aberrant PN size and position have been correlated with developmental arrest and aneuploidy and are represented by PNs of unequal size (>4 μm), localized far apart or peripherally or with the presence of fragmented or additional micronuclei (Munné and Cohen, 1998; Sadowy *et al*., 1998; Garello *et al*., 1999; Nagy *et al*., 2003; Scott *et al*., 2007). Panel experts also agreed and strongly advised that the assessment and elimination of dysmorphic zygotes with smooth endoplasmic reticulum (SER) discs (see Chapter One) due to the association with severely adverse clinical outcomes (Otsuki *et al*., 2004; Ebner *et al*., 2008).

Correct alignment of PNs onto the polar axis is considered a fundamental feature for the completion of the first cleavage division and normal sequential development (Gardner, 1996, 1999, 2001; Edwards and Beard, 1997, 1999; Payne *et al*., 1997; Garello *et al*., 1999; Scott, 2001). Cell cycle-related dynamics of PN events have led many authors to investigate and correlate the presence, pattern and number of NPBs to embryo developmental potential. As shown for mitotic cells, the inequality in number, size or distribution of NPBs is correlated with abnormal development (Pedersen, 1998). Therefore, the panel experts from the consensus workshop established three categories for PN scoring that are based on the morphology of NPBs and PNs, namely: (i) *symmetrical*, (ii) *non-symmetrical* and (iii) *abnormal* (Alpha Scientists in Reproductive Medicine and ESHRE Special Interest Group of Embryology, 2011). Category 1 includes zygotes presenting with equal numbers and size of NPBs, either aligned at the junction between PNs or scattered in both PNs. Category 2, non-symmetrical, comprises all other patterns including peripherally localized PNs. Category 3, abnormal, includes single NPB ('bull's eye') or total absence of NPBs. The latter were found to be correlated with imprinting errors and delayed onset of functional NPBs and nucleoli formation in animal models (Svarcova *et al*., 2009).

Reports on early cleavage checks have been demonstrated to be a beneficial tool in selecting embryos with high implantation potential and decreased chromosomal anomalies (Sakkas *et al*., 1998; Lundin *et al*., 2001). The consensus opinion on a second, Day 1 observation was to leave the choice to the operator's discretion, but if applied, is to be performed 26 ± 1 and 28 ± 1 h post-insemination for ICSI and IVF embryos, respectively.

Sequential morphology assessment through time-lapse cinematography will certainly shed light on the discrepancies in the literature with respect to PN scoring and an in-depth analysis and correlation with the clinical background behind the gametes forming the zygote will possibly reveal even more reliable prognostic tools to improve clinical outcomes.

A. Fertilization assessment

A.1 2PN

When assessments are performed 17 ± 1 h post-insemination, taking into consideration that pronuclear formation in IVF zygotes lags ~1 h behind ICSI zygotes, normally fertilized oocytes should be spherical and have two polar bodies and two PNs (Figs 85–87). PNs should be juxtaposed, approximately the same size, centrally positioned in the cytoplasm with two distinctly clear, visible membranes (Fig. 88). The presence of an equal number and size of NPBs aligned at the PN junction has been correlated with increased embryo competence (Tesarik and Greco, 1999; Tesarik *et al*., 2000; Scott, 2003).

Figure 85 A zygote 16.5 h post-ICSI, having small-sized PNs with scattered NPBs and two visible polar bodies (400× magnification). The zona pellucida (ZP) appears regular; some debris is present in the perivitelline space (PVS). The cytoplasm is homogeneous and displays a clear cortical zone. It was transferred resulting in a clinical pregnancy followed by miscarriage.

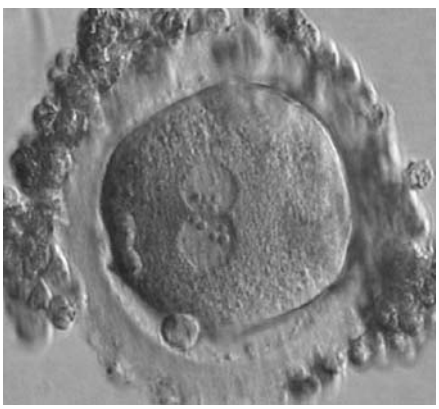

Figure 86 A slightly deformed zygote at 16.5 h after IVF with equal numbers of large-sized NPBs aligned at the PN junction (400× magnification). A great angle separates the two polar bodies. Some granulosa cells surround the ZP. It was transferred but failed to implant.

Figure 87 A zygote at 18.5 h generated by standard insemination using frozen/thawed ejaculated sperm (400× magnification). The two PNs are centrally located: one is slightly larger than the other. NPBs are of the same size, but different in number and are aggregated at adjadjacent borders of each PN. The ZP appears thick. It was transferred but failed to implant.

Figure 88 A zygote generated by ICSI with NPBs perfectly aligned at the junction of centrally located and juxtaposed PNs (600× magnification). Fragmented polar bodies are located in the longitudinal axis of the PNs. Category 1 (equivalent to Z1 score; Scott, 2003) was assigned following assessment. Debris appears to be present in the PVS. The cytoplasm is light-coloured with a clear cortical zone. It was transferred and implanted.

A.2 1PN

The incidence of one pronucleates is around 1% after IVF or ICSI and may be parthenogenetic in origin as suggested by chromosomal analysis that shows a haploid set in approximately half of the studied oocytes (Plachot, 2000). In some cases, only one polar body is extruded into the perivitelline space (PVS) (Fig. 89).

The presence of 1PN can also be a result of errors in the fertilization process with asynchrony in PN formation or PN fusion. In these cases, the resulting oocyte could have a diploid set of chromosomes, and two polar bodies are normally observed (Figs 90–93). The transfer of these oocytes could be considered, but the incidence of aneuploidy in the

Figure 89 A single pronucleate oocyte displaying only one PN and a single polar body observed 16 h post-ICSI (200× magnification). The observation was repeated 17.5, 20 and 22 h post-ICSI and did not show significant variation in the PN size or position.

Figure 90 A zygote observed 15 h post-IVF displaying a single, large-sized PN and two polar bodies (400× magnification).

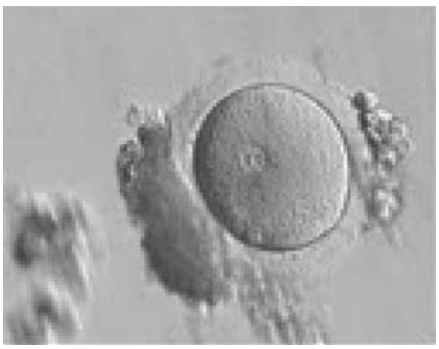

Figure 91 A zygote 17 h post-IVF showing a single PN with NPBs of different size and two polar bodies (400× magnification).

Figure 92 A single, large PN and two polar bodies (partially overlapping) are present in this oocyte observed 16 h and 45 min post-IVF (400× magnification). Four large-sized NPBs are visible. The resulting embryo was transferred, but failed to implant.

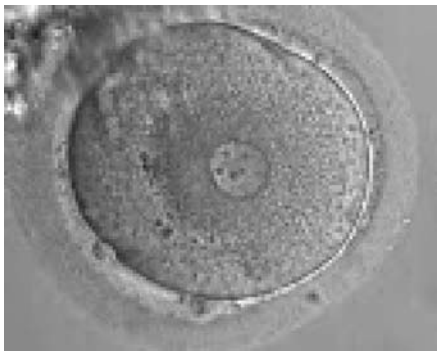

Figure 93 A zygote generated by ICSI showing a single PN and two polar bodies separated by some distance (600× magnification).

Figure 94 A zygote generated by ICSI displaying four PNs of approximately the same size and two of smaller size (150× magnification). Only one polar body is visible.

resulting embryos has been reported to be significantly higher compared with embryos derived from 2PN oocytes (Yan *et al.*, 2010).

A.3 ≥3PN

The formation of triploid zygotes differs in origin, depending on whether they are generated by ICSI or IVF. Only 1% of oocytes after ICSI result in tripronuclear zygotes and are digynic due to failure in extrusion of the second polar body (Fig. 94). An exception is represented by giant oocytes (Fig. 95) that follow different patterns of extrusion due to their generally diploid condition (see Chapter One).

Diandry is the most probable cause of tripronucleates following IVF and occurs in ~5% of inseminated oocytes (Fig. 96). This condition arises from the entry of two spermatozoa into the cytoplasm owing to the incapacity of the oocyte to trigger protection against polyspermy. The second polar body is normally extruded and cleavage often occurs. In some cases, the presence of multiple PNs could be due to failed cytokinesis (Figs 94 and 97) or to penetration by a binucleate spermatozoon (Fig. 98).

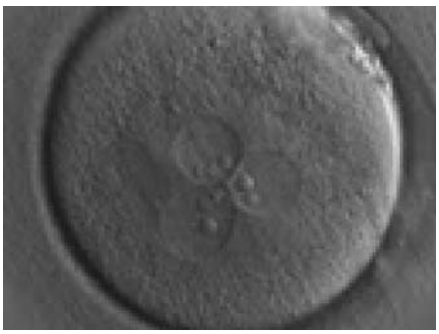

Figure 95 A zygote displaying 3PNs with large-sized NPBs (400× magnification). One of the three PNs is slightly bigger than the others. The zygote was generated by ICSI performed on a giant oocyte.

Figure 96 A zygote displaying 3PNs of approximately the same size with large-sized NPBs, partly overlapped and aligned in the middle of the oocyte (400× magnification). It was generated by IVF and shows two polar bodies.

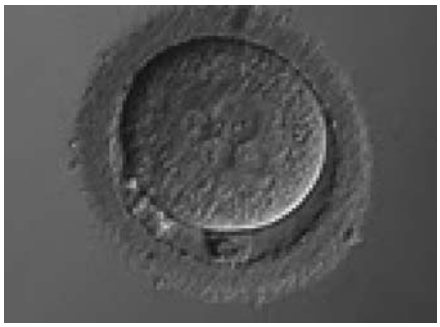

Figure 97 A zygote with 5PNs, halo cytoplasm, fragmented polar bodies, oval shape and dark ZP (400× magnification). It was warmed after vitrification.

Figure 98 A zygote displaying 3PNs after IVF with a small fragment adjacent to the PNs (200× magnification). There are two polar bodies in a large PVS and a thick ZP.

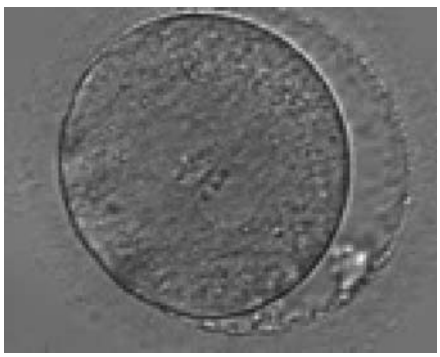

Figure 99 A zygote observed 18 h post-ICSI (400× magnification). The 2PNs are centrally located and juxtaposed in the cytoplasm (peripherally granular), of approximately the same size, and exhibit inequality in the number and size of NPBs. The PN on the right demonstrates fewer but larger nucleoli. Some debris appears to be present in the slightly increased PVS. Transferred on Day 3 (eight cells) along with two other embryos to a patient who delivered a healthy baby boy.

B. Pronuclear size

B.1 Normal

Some studies have demonstrated that the size of PNs depends on gamete factors. Decondensation of the tightly compacted sperm chromatin is a crucial step in fertilization that includes the replacement of protamines with histones under the control of oocyte-decondensing factors. Therefore, the male PN size depends both on the sperm nuclear structure and on the oocyte's capacity of inducing decondensation by releasing appropriate levels of glutathione.

PNs normally appear to be similar in size, although the female PN that is often located towards the second polar body can be slightly smaller (Figs 99 and 100). However, PN formation and rotation is a dynamic process as demonstrated by time-lapse video recording, so positioning and morphology of PNs are strictly time dependent (Fig. 101).

B.2 Small

The size of PNs depends on the time of observation with an increase in size of close to 50% from abuttal to 17 h post-ICSI (Payne *et al.*, 1997). The presence of PNs with a diameter smaller than normal (Figs 102–104) at the normal time of fertilization check could be an indicator of delayed fertilization possibly due to oocyte immaturity, or defects in the gametes. Nevertheless, implantation can occur as a result of transfer of these zygotes (Fig. 103).

B.3 Differential in size

Significant differences (>4 μm) between PN size (Figs 105–108), or the presence of micronuclei or fragmented PNs (Figs 109 and 110) are considered to be abnormal and are associated with chromosomal abnormalities and major loss of developmental potential (Munné and Cohen, 1998; Scott *et al.*, 2000; Nagy *et al.*, 2003; Scott *et al.*, 2007; Alpha Scientists in Reproductive medicine and ESHRE Special Interest Group of Embryology, 2011). Clinical studies have shown a high correlation between zygotes observed at 16–18 h post-insemination displaying large differences in PN size and their capability to maintain viability and development both *in vivo* and *in vitro* (Sadowy *et al.*, 1998; Scott *et al.*, 2000). Therefore, when performing embryo selection these embryos should be avoided for transfer.

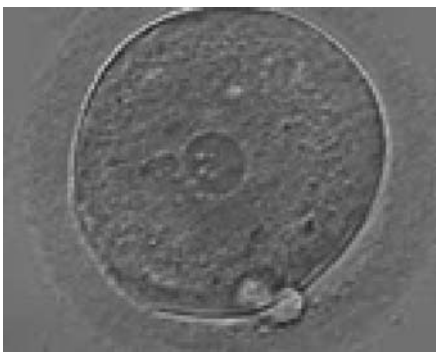

Figure 100 A zygote with equal numbers of large-sized NPBs scattered with respect to the PN junction (400× magnification). PNs are juxtaposed and slightly eccentric. The two polar bodies are located in a plane that is parallel to the longitudinal axis of the PNs.

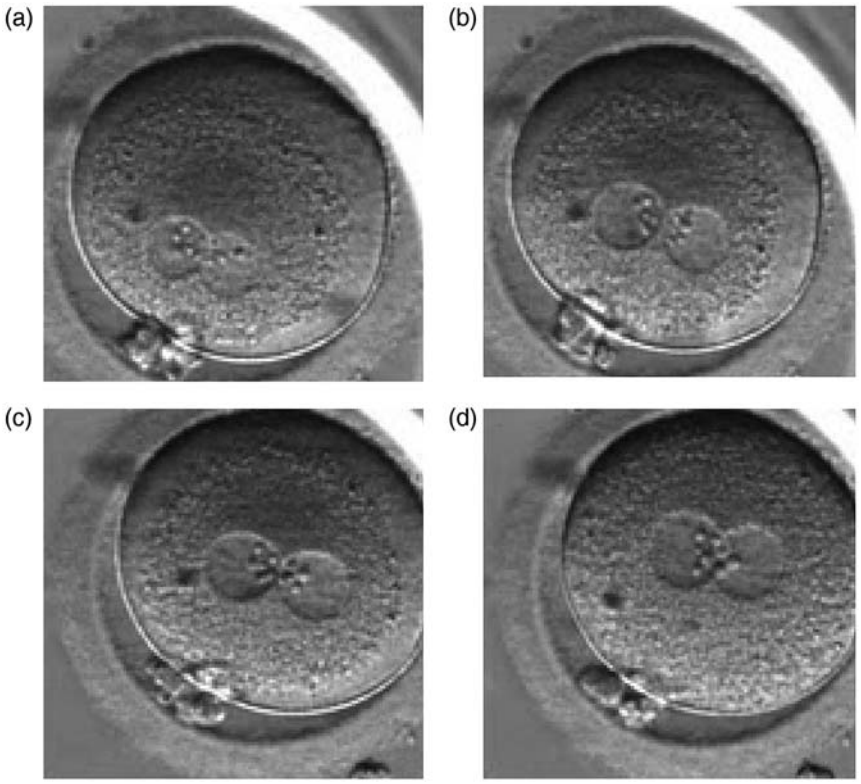

Figure 101 A zygote with changes in PN pattern, particularly with respect to the position in the cytoplasm and the NPBs' location over time at (**a**) 11.7, (**b**) 15.4, (**c**) 18.3 and (**d**) 28.3 h after ICSI (400× magnification).

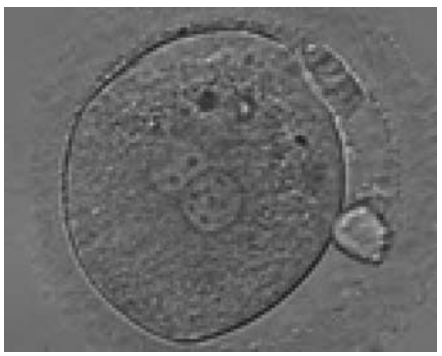

Figure 102 A zygote generated by ICSI and observed 18 h post-insemination (400× magnification). PNs are slightly smaller than normal and exhibit inequality in the number and the distribution of NPBs. Polar bodies are larger than the normal size.

Figure 103 A zygote generated by IVF using frozen/thawed ejaculated sperm and observed 16 h post-insemination (400× magnification). PNs are smaller than normal and are not exactly positioned in the centre of the oocyte. Small-sized NPBs are aligned at the PN junction. It was transferred and implanted.

C. Pronuclear morphology

C.1 Alignment parallel/tangential to the plane of the polar bodies

With the extrusion of the second polar body, following sperm entry and oocyte activation, the polar axis is established. Correct alignment of PNs onto this axis is necessary for the formation of polar axes at syngamy and subsequent completion of the first cleavage division and normal development (Edwards and Beard, 1997; Payne *et al.*, 1997; Garello *et al.*, 1999; Gardner, 2001; Scott, 2001). At apposition, the chromatin of both PNs begins to polarize and rotate to face each other with the male PN rotating onto the female PN and placing the

Figure 104 A zygote displaying two small PNs partly overlapping in this view (600× magnification). NPBs are large in size, equal in numbers and scattered in the two PNs. The ZP appears thickened and the PVS almost absent.

Figure 105 A zygote observed 18 h post-ICSI displaying very unequal-sized juxtaposed PNs, with the smaller PN being less visible (200× magnification). Two polar bodies and small-sized NPBs are scattered in both PNs.

Figure 106 A zygote displaying two polar bodies and unequal-sized juxtaposed PNs and inequality in number and alignment of small-sized NPBs (200× magnification).

Figure 107 A zygote observed 18 h post-insemination displaying very unequal-sized PNs and inequality in number and alignment of NPBs (400× magnification). It was transferred on Day 3 (seven cells) along with two other embryos. The implantation result is therefore unknown. However, the patient delivered a healthy baby boy.

Figure 108 A zygote generated by ICSI with one large and one normal-sized PN (200× magnification). The two polar bodies are at opposite sides of the oocyte.

Figure 109 A zygote after PB biopsy showing peripheral PNs that are very different in size with one larger and one smaller than the normal size (400× magnification). The ZP is oval in shape.

centrosome into the furrow between the two PNs (Van Blerkom *et al.*, 1997). In this way, the longitudinal axis of PNs is parallel to the plane of polar bodies (Figs 111–115). Further rotation brings the PNs aligned onto the polar axis; the position of the second polar body defines the plane of the first cleavage division (Figs 116–121). All these movements and rotations could cause the formation of the clear cortical zone known as the halo (Figs 114, 118 and 119).

C.2 Large angle between polar bodies

The failure of PNs to be juxtaposed and centrally positioned within the cytoplasm or having non-aligned polar bodies with respect to PNs at fertilization check could result in altered development, i.e. fertilization failure and abnormal cleavage of the embryo (Gianaroli *et al.*, 2003; Alpha Scientists in Reproductive medicine and ESHRE Special Interest Group of Embryology, 2011). Large angles between polar bodies (Figs 122–124) have been suggested to be predictors of poor embryo development (Gianaroli *et al.*, 2003). This effect could be due to sub-optimal orientation of PNs (Figs 125 and 126) generating

Figure 110 A zygote 18 h post-ICSI displaying very unequal-sized, juxtaposed PNs and inequality in number and alignment of NPBs (600× magnification). A vacuole-like structure is present in the cytoplasm. Fragments are visible in the PVS, not easily discernible from the polar bodies in this view.

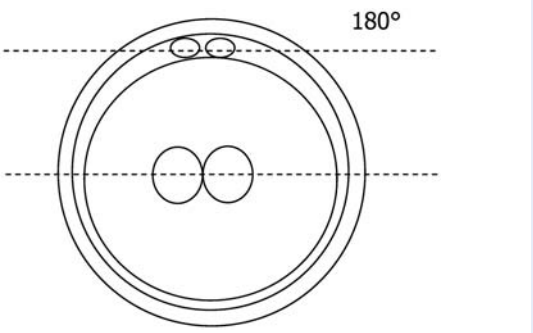

Figure 111 Diagram showing the plane through the polar bodies which is parallel to the contrasting plane through the longitudinal axis of the PNs.

Figure 112 A zygote generated by ICSI with different number of large-sized NPBs aligned at the PN junction (200× magnification). PNs are juxtaposed and centralized; polar bodies are located parallel to the longitudinal axis through the PNs.

Figure 113 An ICSI zygote with large-sized NPBs aligned at the PN junction (200× magnification). PNs are juxtaposed and centralized, fragmented polar bodies are located parallel to the longitudinal axis through the PNs (±30°).

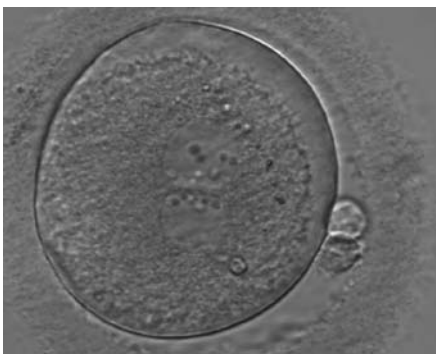

Figure 114 An ICSI zygote displaying juxtaposed and centralized PNs. PN alignment is parallel to the plane of the polar bodies. The zygote displays inequality in number and alignment of NPBs. The latter are aligned in one PN and scattered in the other one with respect to the PN junction. A clear cortical zone with some inclusion bodies immediately below the area can be noted. It was replaced on Day 3 (eight cell cleavage embryo) but failed to implant.

Figure 115 A zygote with an equal number of large-sized NPBs aligned at the PN junction (400× magnification). PNs are juxtaposed and centralized and the polar bodies are located parallel to the longitudinal axis through the PNs. Observed 16 h after IVF.

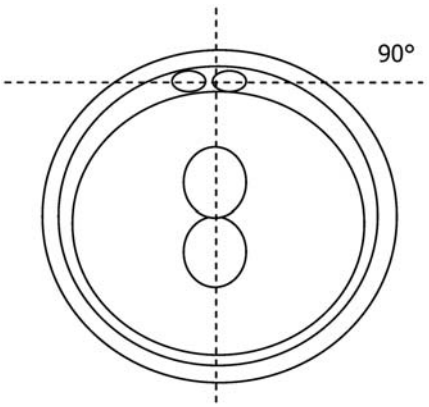

Figure 116 Diagram showing the plane through the polar bodies which is tangential to the contrasting plane through the longitudinal axis of the PNs.

Figure 117 An ICSI zygote with large-sized NPBs aligned at the PN junction (400× magnification). PNs are juxtaposed and centralized; polar bodies (the first polar body is fragmented, the second is intact) are located tangential to the longitudinal axis through the PNs.

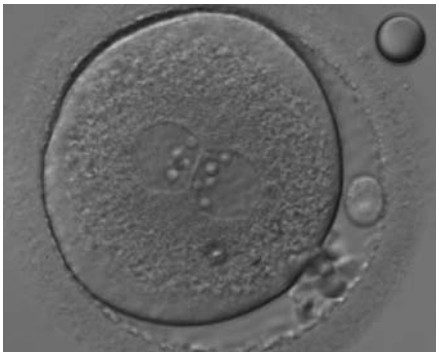

Figure 118 An ICSI zygote with large-sized NPBs aligned at the PN junction (400× magnification). PNs are juxtaposed and centralized; polar bodies (the first polar body is fragmented, while the second is intact) are located tangential to the longitudinal axis through the PNs.

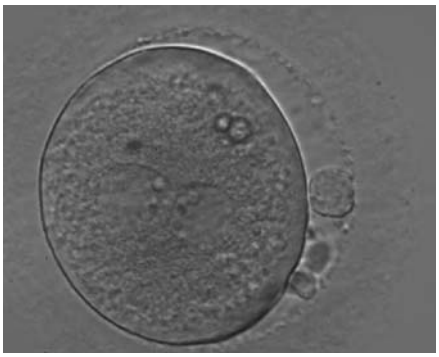

Figure 119 An ICSI zygote with large-sized NPBs aligned at the PN junction (200× magnification). PNs, juxtaposed and centralized, are tangential to the plane through the polar bodies. It was transferred on Day 3 (seven cells) along with two other embryos but failed to implant.

Figure 120 Zygote observed at 16.5 h post-IVF displaying unequal-sized juxtaposed and centralized PNs aligned tangentially to the plane through the polar bodies (400× magnification). NPBs are scattered in one PN and aligned in the other. The oocyte is irregular in shape and the PVS is enlarged. It failed to implant following transfer.

Figure 121 A deformed zygote with peripheral PNs and polar bodies aligned tangentially to the plane through the polar bodies observed 15 h post-IVF (400× magnification). Polar bodies are highly dysmorphic. Note the presence of small vacuoles in the cytoplasm.

Figure 122 An ICSI zygote displaying two PNs of approximately equal size, juxtaposed and clearly visible in the middle of the cytoplasm (400× magnification). Polar bodies are rotated >30° off the longitudinal axis through the PNs. A clear cortical area and coarse granularity of the cytoplasm can be observed. It was transferred but failed to implant.

a great degree of cytoplasmic turbulence, which could facilitate uneven cleavage or fragmentation (Garello *et al*., 1999).

C.3 Abutment/separation between PNs

In human oocytes, the aster from the sperm centrosome organizes the microtubules, which control the abutment and apposition of PNs (Figs 127–131), and direct the formation of polar axes at syngamy by setting the plane of the first division. The subsequent movements and rotations favour the distribution of the mitochondria and chromatin alignment, which are essential for correct development.

Failed progression to apposition and syngamy (Figs 132–134) mostly depends on sperm centrosome activity. Observations of zygotes with separated PNs at fertilization check during subsequent development (Figs 135–136) demonstrate severe delay or arrest in development (Fig. 136) in almost 80% of cases (Gianaroli *et al*., 2003). This condition

Figure 123 Zygote observed 18 h post-ICSI, with inequality in number and alignment of the NPBs (400× magnification). PNs are juxtaposed and centralized, NPBs are aligned in one of the two PNs and scattered in the other with respect to the PN junction. Both polar bodies are rotated >30° off the longitudinal or meridional axis with a large degree of separation between them. It is possible to observe a clear cortical zone and some dark inclusion bodies. It was transferred and failed to implant.

Figure 124 A zygote of irregular shape observed 18 h post-ICSI (400× magnification). The visible PNs show unequal distribution of the NPBs. PNs are juxtaposed and centralized and the polar bodies form a great angle with respect to the longitudinal axis through the PNs. It was transferred but failed to implant.

is most frequently associated with pathological spermatozoa, particularly from epididymal or testicular samples (Fig. 133).

C.4 Centrally/peripherally positioned PNs

The position of PNs has a relevant effect on the first cleavage plane that normally goes through the pronuclear axis (Scott, 2003). In the majority of zygotes with centrally positioned PNs (Fig. 137), the first cleavage occurs regularly, giving rise to normally developing embryos. Due to the dynamics of PN movements within the cytoplasm, their orientation on the polar axis varies depending on the progression of rotation (Figs 138 and 139) towards the final state which determines the first cleavage plane (Fig. 140).

In cases of peripherally positioned PNs (Figs 141and 142), cleavage occurs according to the pronuclear axis and results frequently in

Figure 125 Zygote with large-sized NPBs scattered with respect to the PN junction (400× magnification). A clear cortical zone can be observed in the cytoplasm and the ZP is thick and very dense. Polar bodies form a great angle with respect to the longitudinal axis through the PNs. It was transferred but implantation outcome is unknown.

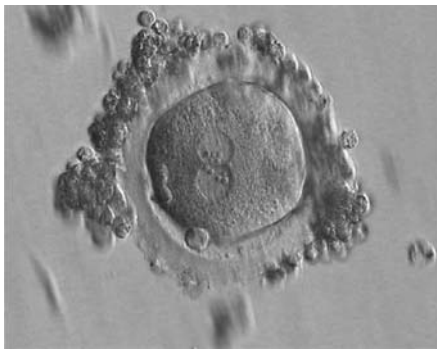

Figure 126 A zygote of irregular shape 16.5 h after IVF in which two PNs are clearly visible with NPBs aligned in both (400× magnification). Polar bodies form a right angle: one is aligned with the longitudinal axis through the PNs and the other is aligned with the meridional axis. It was transferred but failed to implant.

abnormal morphology (Fig. 143), cleavage (Fig. 144) and arrest of development (Fig. 145). Nevertheless implantation can occur (Fig. 146).

C.5 Pronuclear membrane breakdown/ syngamy

Following sperm entry, both PNs migrate toward each other while replicating their own DNA. At juxtaposition, nuclear membranes break down a few hours prior to initiation of the first cleavage division (Figs 147 and 148). Syngamy occurs (Fig. 149) and the two sets of haploid genomes merge.

The astral centrosome containing two centrioles splits and relocates to opposite poles of a bipolar spindle to establish bipolarization that controls cell division. The centrioles take a pivotal position on spindle poles, while chromosomes organize on the equator of the metaphase plate. Anaphase and telophase ensue completing the first mitotic division.

Figure 127 Irregularly shaped zygote showing two centrally located and juxtaposed PNs with equal numbers of large-sized NPBs aligned at the PN junction (200× magnification). Fragmented polar bodies are located parallel to the longitudinal axis through the PNs (±30°). A clear cortical area and coarse granularity of the cytoplasm can be observed. It was transferred on Day 3 along with two other embryos and the patient delivered two healthy baby girls and one healthy baby boy.

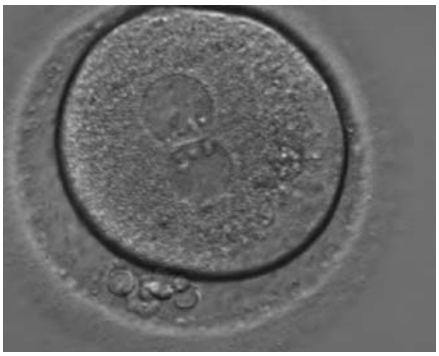

Figure 128 A zygote with two centrally located and juxtaposed PNs, an enlarged PVS and a significant amount of debris in the PVS (400× magnification). It was transferred but the result is unknown.

Figure 129 A zygote with two centrally located and perfectly juxtaposed PNs in a granular cytoplasm with a clear cortical zone (400× magnification). NPBs are aligned, but are different in size. It was transferred but failed to implant.

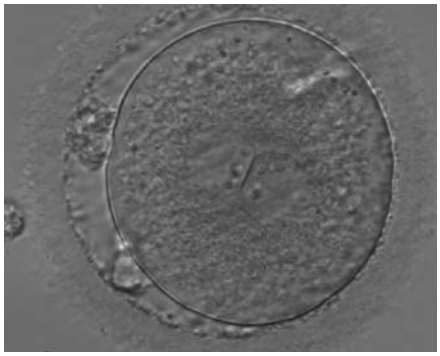

Figure 130 A zygote with two centrally located and perfectly juxtaposed PNs in a slightly granular cytoplasm with a clear cortical zone (400× magnification). There is debris in the PVS as well as fragmentation of one polar body (presumably the first polar body), which is significantly separated from the other polar body (presumably the second polar body). It was transferred but the outcome is unknown.

Figure 131 A zygote generated by IVF with a thick ZP (400× magnification). PNs are juxtaposed in the cytoplasm, which has a clear cortical zone. NPBs are small and aligned in one PN and scattered in the other. A refractile body is visible at the 11 o'clock position in this view.

Figure 132 A zygote 18 h post-ICSI displaying two PNs that are not juxtaposed (200× magnification). NPBs are of different size, aligned in one PN and scattered in the other. The cytoplasm is very granular.

Figure 133 A zygote generated by ICSI using fresh epididymal sperm, observed 18 h post-insemination (400× magnification). PNs are not juxtaposed, different in size and NPBs are symmetrically distributed. It was transferred but failed to implant.

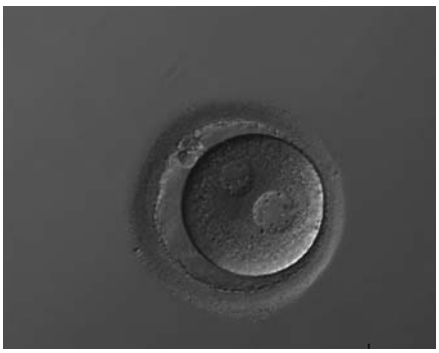

Figure 134 A zygote with widely separated and unequal-sized PNs, which show scattered small NPBs (150× magnification). The cytoplasm appears slightly granular and the PVS is enlarged. It was transferred but implantation outcome is unknown.

Figure 135 A zygote generated by ICSI and observed at 16, 17.5, 19 and 22 h after insemination (200× magnification). The two PNs are peripherally located, widely separated and have an unequal number of scattered NPBs. It was discarded.

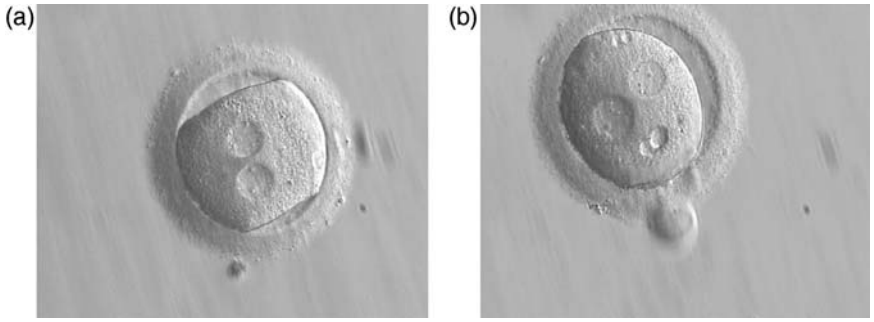

Figure 136 A zygote with an irregular shape, generated by ICSI and observed 18 h **(a)** and 20 h **(b)** post-ICSI (400× magnification). The polar body had been biopsied. PNs are widely separated and contain scattered small NPBs. The cytoplasm is normal in colour but displays two vacuole-like structures which are evident in (b). It failed to cleave during further development.

Figure 137 A zygote displaying centrally located, and in this view, partially overlapping PNs (400× magnification). The PN longitudinal axis is parallel to the polar bodies. NPBs are scattered in both PNs with respect to the PN junction but differ in number. It was transferred and implanted.

Figure 138 A zygote displaying centrally located PNs in which NPBs are symmetrically distributed and aligned with respect to the PN junction (400× magnification). A clear cortical zone, the halo, appears in the cytoplasm and there is a slightly enlarged PVS. It was transferred but implantation outcome is unknown.

Figure 139 A zygote, generated by ICSI and observed 18 h post-insemination displaying centrally located PNs in which NPBs differ in number and size (400× magnification). The PN longitudinal axis is almost tangential to the plane through the polar bodies. NPBs are not symmetrically distributed, aligned in one PN and scattered in the other with respect to the PN junction. The ZP is thick and brush-like. It was transferred and failed to implant.

Figure 140 A zygote with equal numbers of large-sized NPBs aligned at the PN junction (200× magnification). PNs are juxtaposed and centralized; polar bodies are aligned tangential to the longitudinal axis through the PNs.

Figure 141 An ICSI zygote displaying two perfectly juxtaposed PNs in a peripheral position in the cytoplasm, which is showing central granularity due to clustering of the organelles (400× magnification). NPBs are different in number and distribution. One polar body (presumably the first polar body) is fragmented and the other is intact. It was transferred but the outcome is unknown.

Figure 142 A zygote generated by IVF with normal-sized PNs slightly displaced to a peripheral position (400× magnification). NPBs are aligned and different in number. It was transferred but the outcome is unknown.

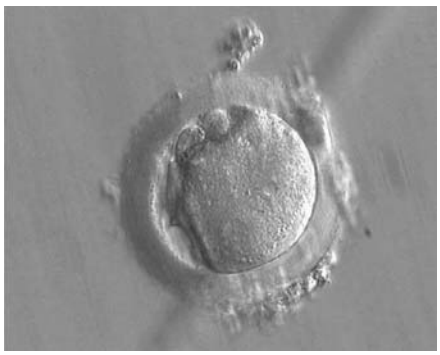

Figure 143 A deformed zygote at 16 h post-IVF displaying two PNs located peripherally in the cytoplasm (6–7 o'clock) that are parallel to the plane of the two large polar bodies (400× magnification).

Figure 144 A zygote observed 16 h post-IVF showing peripheral PNs partly overlapping in this view (400× magnification). NPBs are small in size and scattered in both PNs. The derived embryo was highly fragmented with uneven blastomeres and was discarded.

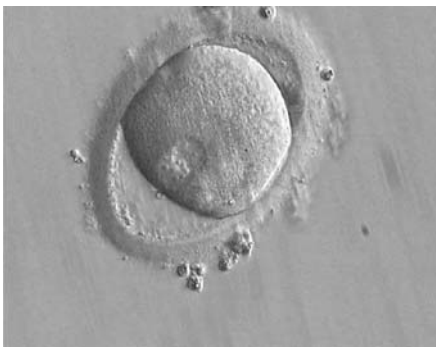

Figure 145 A zygote observed 16 h post-ICSI with peripherally positioned PNs (400× magnification). A large PVS is present inside a deformed, ovoid ZP. The oocyte has a clear cortical zone in the cytoplasm. It was not transferred because of arrested development.

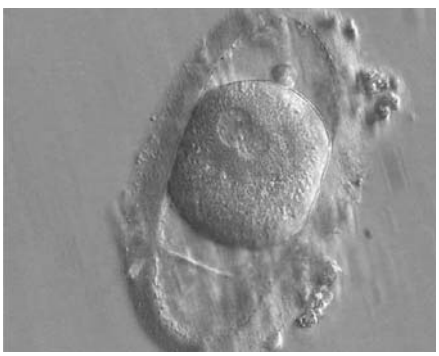

Figure 146 A zygote generated by ICSI displaying an ovoid ZP which demonstrates a duplication or tear in the layers (400× magnification). The fertilized oocyte is spherical and shows two PNs peripherally located and partly overlapping in this view. NPBs are small and scattered in both PNs. It was transferred and implanted.

Figure 147 A zygote entering syngamy observed at 18 h after ICSI (400× magnification). The PN membranes are becoming indistinct and have large-sized NPBs. The ZP appears 'brush-like' and there is a clear cortical region evident in the peripheral cytoplasm. Further development resulted in cleavage to 4 cell and arrest on Day 3.

Figure 148 A zygote which is entering syngamy and is displaying membrane breakdown particularly evident in the upper PN (400× magnification). The observation was performed 15 h after ICSI. One of the two PNs and its associated NPBs are now very indistinct. It was transferred but failed to implant.

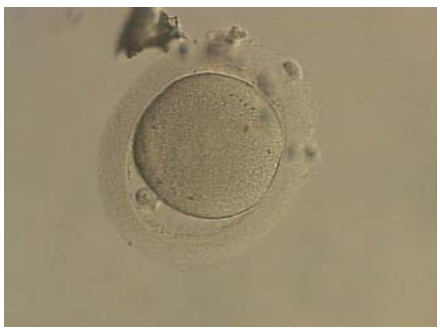

Figure 149 An ICSI zygote which has entered syngamy and is displaying pronuclear membrane breakdown (200× magnification). The NPBs are no longer distinct. It was transferred but the outcome is unknown.

In contrast to some animal species, membrane fusion of PNs (Fig. 150) is not a common process in human zygotes.

D. Nucleolar precursor bodies

D.1 NPBs: aligned/scattered/differential alignment between PNs

As PNs form after fertilization, there is polarized distribution in the chromatin into the furrow between them (Van Blerkom *et al.*, 1997). As NPBs are attached to the chromatin, they should also polarize or align with it implying that, if there is correct chromatin polarization, the NPBs will appear polarized as well (Figs 151–154). Due to the dynamics of this event, some zygotes show symmetry in appearance of the PNs, but a delay in the alignment of the chromatin into

Figure 150 A zygote displaying PNs entering syngamy (400× magnification). The observation was performed 16 h after ICSI. The PN membranes are indistinct, particularly between the PNs where they have broken down, looking like PN membrane fusion. Large-sized NPBs are evident in the PNs. Polar bodies had been previously biopsied. It was transferred but failed to implant.

Figure 151 A zygote observed 18 h post-ICSI with equal numbers of NPBs aligned at the PN junction (200× magnification). It was transferred but the outcome is unknown.

Figure 152 A zygote observed 18 h post-ICSI with equal numbers of NPBs aligned at the PN junction (200× magnification). It shows a large PVS and an irregular ZP. The polar bodies are fragmented and overlapping in this view. It was transferred but the outcome is unknown.

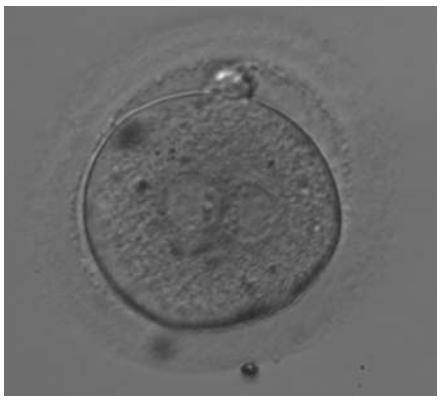

Figure 153 A zygote observed 18 h post-ICSI with NPBs aligned at the PN junction (200× magnification). NPBs differ in number and size between PNs. The polar bodies are overlapped in this view. It was discarded due to subsequent abnormal cleavage.

the furrow, or onto the mitotic plate (Figs 155–157). NPB and PN progression can occur even in highly dysmorphic zygotes (Fig. 158).

During the progression of the cell cycle, NPBs change in number, size and distribution (Fig. 101) and finally they disappear shortly before syngamy and initiation of the first cleavage division (Fig. 149). Recent investigations by time-lapse imaging have shown that NPBs are highly dynamic and that a characteristic NPB pattern may change within a short period of time (Montag *et al*., 2011).

The potential use of the arrangement of NPBs in both PNs regarding size, number and symmetry was initially investigated as a major part of PN scoring in the late 90s (Scott and Smith, 1998). Several publications found a benefit of PN scoring and especially the distribution of NPBs with the outcome of assisted reproduction treatment (Tesarik

Figure 154 A zygote generated by ICSI, displaying two perfectly juxtaposed PNs within which the NPBs are aligned, have the same size and are similar in number (400× magnification). It was transferred but the outcome is unknown.

Figure 155 An ICSI zygote with large-sized NPBs scattered with respect to the PN junction (400× magnification). The cytoplasm appears granular. It was transferred but failed to implant.

Figure 156 An ICSI zygote with NPBs scattered with respect to the PN junction (400× magnification). Polar bodies are fragmented; there is debris in the PVS. It was transferred but implantation outcome is unknown.

Figure 157 An ICSI zygote displaying partially overlapping PNs in this view. NPBs are scattered in both PNs (400× magnification). It was transferred but the outcome is unknown.

Figure 158 A zygote generated by IVF at 16.40 h post-insemination (400× magnification). It shows small-sized NPBs scattered with respect to the PN junction and a lot of large cellular debris in the PVS. It was discarded.

and Greco, 1999; Scott *et al*., 2000; Balaban *et al*., 2001; Montag and van der Ven, 2001; Ebner *et al*., 2003; Senn *et al*., 2006). Others have reported no benefit (Payne *et al*., 2005; James *et al*., 2006; Nicoli *et al*., 2007; Brezinova *et al*., 2009).

NPBs' morphology is influenced by the patient's age and there is also a temporal difference in morphology between zygotes from IVF compared with ICSI. Therefore, comparative PN/NPB scoring should be performed according to strict guidelines considering timing, patient characteristics and insemination technique employed.

Many cell cycle control proteins are located in the nucleolus, and it has been shown in mitotic cells that asymmetry in number and pattern of NPBs is associated with abnormal cell cycles and ultimately with abnormal development (Pedersen, 1998). It is plausible that asymmetry between PNs in zygotes (Figs 159–162) can lead to abnormal development with an increase in fragmentation and abnormal cleavage, and reduced viability (Scott, 2003). Nevertheless, implantation can occur (Figs 163 and 164).

Pronuclear scoring based on Scott's (2003) Z scores, which combines the assessment of PN orientation and NPB pattern, was

Figure 159 A zygote with inequality in numbers and alignment of NPBs. It was cryopreserved.

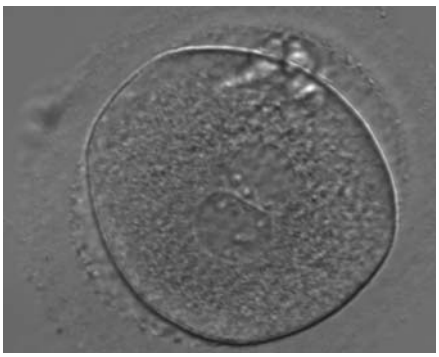

Figure 160 A zygote generated by ICSI with inequality in numbers and alignment of NPBs (400× magnification). NPBs are aligned in one PN and scattered in the other. Due to poor development, it was discarded.

Figure 161 A zygote generated by IVF with inequality in numbers and alignment of NPBs (600× magnification). It was discarded.

Figure 162 A zygote observed 16 h post-ICSI with small-sized NPBs scattered with respect to the PN junction in both PNs (400× magnification). It has a very thin ZP. It was transferred but failed to implant.

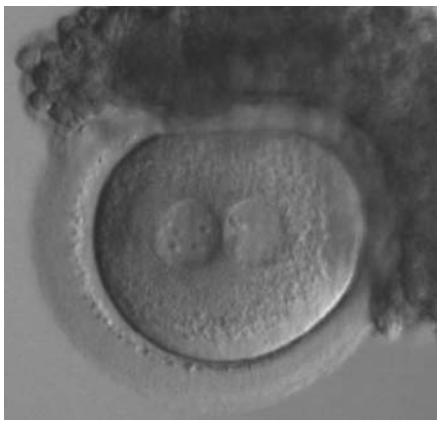

Figure 163 A zygote generated by ICSI with inequality in numbers and alignment of NPBs (200× magnification). Many granulosa cells are adherent to the ZP. It was transferred and implanted.

Figure 164 A zygote at 15 h post-IVF in which NPBs are scattered in one of the two PNs and aligned in the other (400× magnification). The ZP is thick and the PVS is enlarged. One of the two polar bodies is fragmented. It was transferred and implanted.

Figure 165 A zygote generated by ICSI with equal numbers of large-sized NPBs aligned at the PN junction (200× magnification). It was transferred but the outcome is unknown.

adopted by the consensus workshop (Alpha Scientists in Reproductive medicine and ESHRE Special Interest Group of Embryology, 2011) but modified into three categories:

(i) symmetrical PNs (corresponding to Scott's Z1 and Z2)
(ii) non-symmetrical PNs (other arrangements, peripheral PNs)
(iii) abnormal PNs (PNs with none or one NPB, which are called respectively 'ghost' PNs and 'bulls-eye' PNs. Both have been associated with abnormal outcome in animal models.

D.2 Numbers similar/numbers different between PNs

Human cells generally have two to seven nucleoli per human nucleus with equal numbers in the two daughter cells after a mitotic division. Nucleoli appear and disappear depending on the cell cycle phase: they are more numerous at the G1 phase, then start to fuse, and at the S1 phase there are only one to two large nucleoli per nucleus. When asynchrony occurs, this appears to be the result of aberrant chromosomal function.

Transferring this model to the zygote, the ideal oocytes are those presenting with symmetry for number and size of NPBs that are aligned on the furrow between the 2PNs (Figs 165–167). Equality in number with non-alignment in both PNs is also indicative of synchronised development (Fig. 168). In contrast, any form of disparity in NPBs' size, number or pattern of alignment between the PNs, is associated with a poor outcome (Figs 169–172).

D.3 Similar size of NPBs/different size of NPBs

The dynamics of nucleoli formation associated with NPBs merging implies a time-related change in NPBs' size (Scott, 2003). A progressive increase in NPBs' size and a concomitant reduction in number

Figure 166 A zygote generated by ICSI with equal numbers of large-sized NPBs aligned at the PN junction (400× magnification). There is a halo in the cortical area; polar bodies are fragmented and the ZP appears brush-like. It was discarded due to subsequent abnormal development.

Figure 167 A zygote generated by IVF observed 17 h post-insemination (400× magnification). PNs have similar numbers of large-sized NPBs aligned at the PN junction. The PVS is slightly enlarged and the ZP is normal in size and surrounded by some granulosa cells. It was transferred but failed to implant.

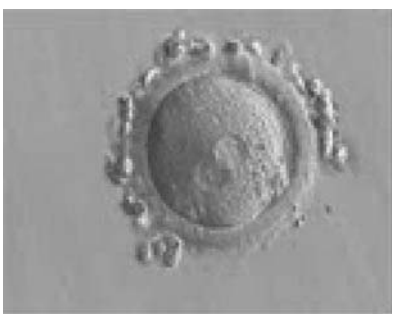

Figure 168 A zygote generated by IVF using frozen/thawed ejaculated sperm and observed 15 h post-insemination (400× magnification). Two PNs of approximately the same size are clearly visible in the cytoplasm. Peripheral granular cytoplasm can be seen. NPBs are scattered in both PNs. Both polar bodies are located at the 4 o'clock position. It was transferred and implanted.

Figure 169 A zygote generated by ICSI showing different numbers of NPBs (400× magnification). The cytoplasm appears granular. It was transferred but failed to implant.

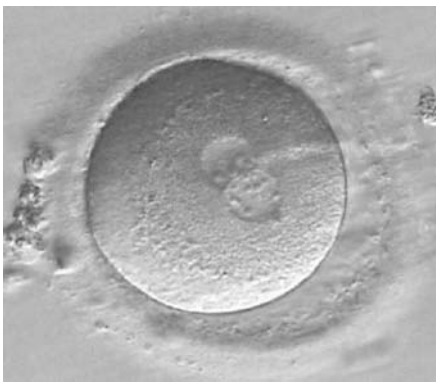

Figure 170 A zygote observed 16.5 h post-ICSI, showing unequal number and size of NPBs: medium-sized and scattered in one PN, larger-sized and aligned in the other (400× magnification). Polar bodies had been biopsied, and the slit opened mechanically in the ZP is evident at the 3 o'clock position. It was cryopreserved.

Figure 171 A zygote observed at 16 h post-IVF displaying different number and size of NPBs: small and scattered in one PN, large and aligned in the other (400× magnification). It was discarded because of developmental arrest.

occur at the time of nucleoli alignment into the furrow between PNs (Figs 173–176).

The presence of small scattered and unequal-sized NPBs (Figs 177–179) could be indicative of functional defects in nucleoli with consequent decreased or ineffective synthesis of rRNA. The extent of malfunctioning possibly depends on the grade of asynchrony and on the number of affected nucleoli as demonstrated by the clinical outcome that may result in implantation (Fig. 180).

D.4 Ghost PNs (absent NPBs)/single NPB in one or more PNs (bull's eye)

Despite the difficulty of making comparative studies aimed at evaluating the relevance of PN scoring, the sequence of processes involved in fertilization underlines the importance and significance of NPBs and

Figure 172 A zygote generated by ICSI with a different number and size of scattered NPBs (600× magnification). It was discarded because of subsequent abnormal development.

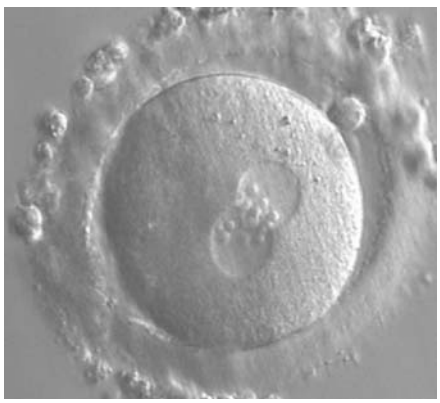

Figure 173 A zygote generated by ICSI showing equal number and size of NPBs, which are aligned at the PN junction (200× magnification). PNs are tangential to the plane of the polar bodies. It was transferred and resulted in a singleton pregnancy and delivery.

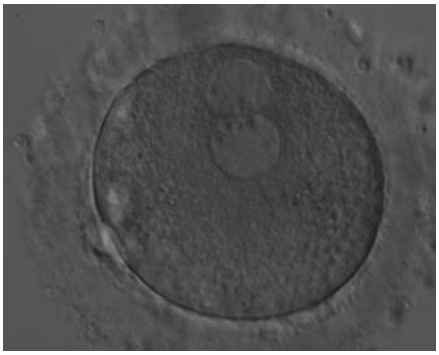

Figure 174 A zygote generated by ICSI with peripherally located PNs showing NPBs of similar size and number (200× magnification). Further development resulted in uneven cleavage and arrest on Day 3.

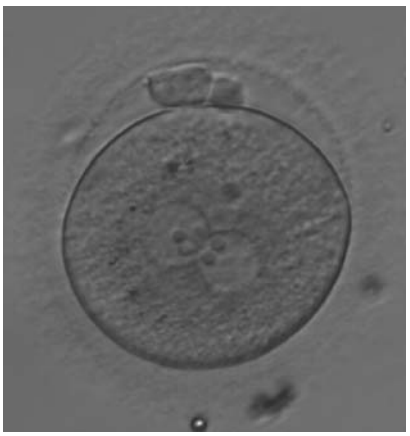

Figure 175 A zygote observed at 18 h after ICSI, with NPBs of equal size in both PNs and aligned at the PN junction (200× magnification). Polar bodies are intact and slightly larger than normal. The cytoplasm is granular with some inclusions. It was discarded due to subsequent abnormal development.

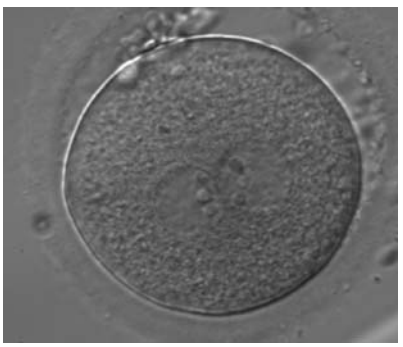

Figure 176 A zygote generated by ICSI showing equal number and size of NPBs, which are perfectly aligned at the PN junction (200× magnification). Polar bodies are highly fragmented. It was transferred but clinical outcome is unknown.

Figure 177 A zygote generated by ICSI displaying unequal number and size of NPBs between the PNs (400× magnification). It was transferred but clinical outcome is unknown.

Figure 178 A zygote generated by ICSI showing an unequal number of NPBs (400× magnification). The NPBs differ in size within each PN. It was transferred but clinical outcome is unknown.

Figure 179 A zygote generated by ICSI displaying unequal number and size of NPBs between the PNs (400× magnification). NPBs are mainly aligned at the PN junction. It was transferred but clinical outcome is unknown.

nucleoli in determining embryo viability. In light of these considerations, it is not surprising that the absence of nucleoli in PNs at the time of fertilization check, the so-called 'ghost' PNs (Figs 181–184), or the presence of a single NPB, known as 'bull's eye' PNs (Figs 185–189) has been reported to be associated with epigenetic defects and abnormal development in animals (Svarcova *et al.*, 2009).

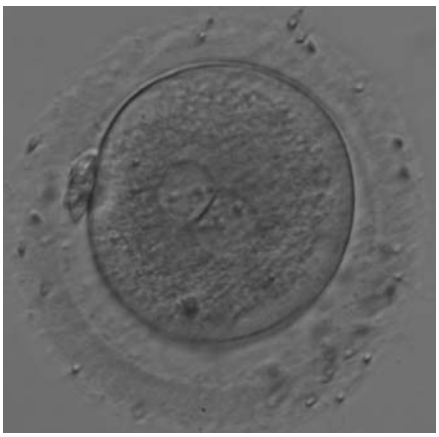

Figure 180 A zygote generated by IVF with large NPBs scattered with respect to the PN junction (200× magnification). NPBs display differences in sizes within each PN and are slightly larger in the PN on the right side. It was transferred and resulted in a singleton pregnancy with delivery.

Figure 181 One out of three sibling zygotes (see also Figs 182 and 183) generated by ICSI using frozen/thawed epididymal sperm observed 18 h post-insemination. All three zygotes clearly show two distinct PNs with well-defined membranes and without any NPBs. All three were transferred and two healthy baby boys were delivered.

Figure 182 The second out of three sibling zygotes (see also Figs 181 and 183) generated by ICSI using frozen/thawed epididymal sperm. All three zygotes showed refractile bodies in the cytoplasm.

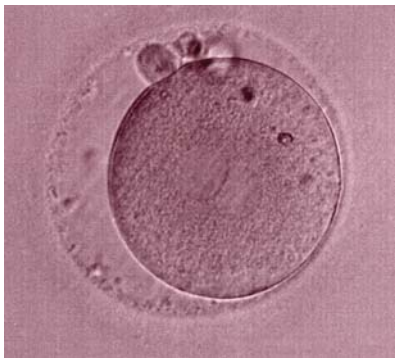

Figure 183 The third of three sibling zygotes (see also Figs 181 and 182) generated by ICSI using frozen/thawed epididymal sperm. Beside the absence of NPBs and the presence of refractile bodies, this zygote has a large perivitelline space.

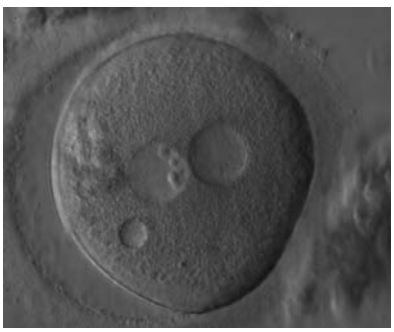

Figure 184 A zygote generated by ICSI showing what looks like two distinct PNs with distinct membranes and the absence of NPBs in one of the PNs (400× magnification). One small vacuole is visible under the left PN. Two highly fragmented polar bodies are present at 9 o'clock. Despite the presence of 2 polar bodies after ICSI, it is possible that this is a 1PN zygote, and that the structure to the right is a vacuole (compare with Fig. 209). It was not transferred.

Figure 185 A zygote generated by ICSI showing two 'bull's eye' PNs, each having a single large NPB (200× magnification). The PNs are slightly separated and are not as yet juxtaposed. A clear cortical region is evident in the cytoplasm. It was discarded.

Figure 186 Oval-shaped zygote generated by ICSI, showing a single NPB in one of the two PNs ('bull's eye') and small, scattered NPBs in the other (200× magnification). The PVS is quite large and the polar bodies are highly fragmented. It was discarded.

Figure 187 Zygote generated by ICSI with one 'bull's eye' NPB in one PN and small, different-sized NPBs in the other (400× magnification). It was transferred but clinical outcome is unknown.

Figure 188 Zygote generated by ICSI displaying two centrally positioned PNs: in one PN there is a single large NPB ('bull's eye'), whereas the NPBs are smaller, different-sized and scattered in the other (600× magnification). It was discarded.

Figure 189 A zygote generated by ICSI with one 'bull's eye' PN (400× magnification). The NPBs from each PN are aligned at the PN junction. It was transferred but clinical outcome is unknown.

E. Cytoplasmic morphology assessment

E.1 Normal/granular

Homogeneous cytoplasm is expected in zygotes as for oocytes (Figs 190 and 191), but heterogeneous cytoplasm is of unknown developmental significance. Therefore, although some studies have reported that severe cytoplasmic anomalies in the zygote adversely affect the developmental and implantation potential of the resulting embryo (Kahraman *et al.*, 2000; Ebner *et al.*, 2003; Balaban and Urman, 2006), there is no clear evidence supporting these findings. Similarly, the presence of a peripheral cytoplasmic translucency in the fertilized oocyte (known as the 'halo'; Fig. 192) or of minor dysmorphisms such as debris in the PVS (Fig. 193) or presence of refractile bodies in the cytoplasm (Fig. 194) have not been proved to be of

Figure 190 A zygote generated by IVF with frozen/thawed ejaculated sperm and observed at 16 h post-insemination showing normal cytoplasmic morphology (400× magnification). NPBs are obviously different in the two PNs. It was transferred but failed to implant.

Figure 191 A zygote generated by ICSI, which subsequently underwent polar body biopsy, shows normal cytoplasmic morphology (400× magnification). It was discarded due to aneuploidy.

Figure 192 A zygote generated by IVF with frozen/thawed ejaculated sperm and observed at 16 h post-insemination showing normal cytoplasmic morphology with an evident clear cortical zone, the halo, in the cytoplasm (400× magnification). NPBs are scattered and different-sized, polar bodies are fragmented. It was cryopreserved.

Figure 193 A zygote generated by ICSI showing normal cytoplasmic morphology, a thin ZP and small debris in an enlarged PVS (400× magnification). It was transferred but clinical outcome is unknown.

Figure 194 A zygote generated by ICSI showing normal cytoplasmic morphology except for a refractile body visible at the 3 o'clock position in this view (400× magnification). It was transferred but clinical outcome is unknown.

prognostic value for implantation. Nevertheless, recording of these observations should be made as the accumulation of data could reveal some relevant links to developmental or implantation potential.

Normal cytoplasm is clearly distinguishable from granular cytoplasm, but to make comparative observations attention should be paid to the optical system and culture medium employed. The severity of granularity is generally based on the diameter and depth of the granular area that may occupy either the whole zygote (Fig. 195), or small (Figs 196–198) or large areas of the cytoplasm (Figs 199 and 200).

It has been reported that half of the oocytes with dysmorphic phenotypes such as organelle clustering are aneuploid, with hypohaploidy being the predominant abnormality (Van Blerkom and Henry, 1992). This severe cytoplasmic disorganization is associated with a lower intracytoplasmic pH and decreased ATP content (Van Blerkom *et al*., 1997). These dysmorphic changes would be inherited in the zygote. Apparently, intracytoplasmic organelle clustering (Fig. 200) is a type of severe abnormality that is significantly repetitive in consecutive cycles and is a negative predictor of pregnancy and implantation

Figure 195 A zygote generated by ICSI displaying heterogeneous, granular cytoplasm (200× magnification). NPBs are large-sized and polar bodies are fragmented. It was discarded due to poor subsequent development.

Figure 196 A zygote generated by IVF using frozen/thawed ejaculated sperm and observed at 17 h post-insemination showing an irregular oolemma and dysmorphic granular cytoplasm (400× magnification). PNs are different in size and peripherally located. NPBs differ in size and number between PNs. It was transferred but failed to implant.

Figure 197 A zygote generated by ICSI with peripheral PNs (150× magnification). The oolemma is irregular and the cytoplasm is dysmorphic and granular. The ZP is thick and dark. It was discarded.

Figure 198 A zygote generated by ICSI displaying granular cytoplasm, especially in the area immediately adjacent to the clear cortical zone (400× magnification). There is an enlarged PVS and an ovoid ZP. NPBs differ in number and size. It was transferred but clinical outcome is unknown.

Figure 199 A zygote generated by ICSI with four PNs (possibly a result of fragmentation of an originally normal-sized PN), displaying very granular cytoplasm and a clear cortical zone (600× magnification). It was discarded.

Figure 200 A zygote generated by ICSI using frozen/thawed ejaculated sperm (200× magnification). PNs are peripherally located with a large inclusion positioned directly below the PNs that is displaying a crater-like appearance as a consequence of severe organelle clustering. It was discarded.

rates, although the cleavage stage embryo quality, as observed by light microscopy, is apparently not affected (Meriano *et al.*, 2001).

E.2 Small vacuoles/large vacuoles

The presence of a few small vacuoles (diameter of 5–10 μm) that are apparently fluid filled and transparent (Figs 201 and 202) have not been associated with detectable biological consequences, but some concern may arise when several vacuoles appear (Figs 203 and 204) or appear with other morphological anomalies (Fig. 205).

Large vacuoles (>14 μm in diameter) in fertilized oocytes (Figs 206–210) can interfere with cleavage planes, resulting in reduced blastocyst formation (Ebner *et al.*, 2005). For this reason, they are normally not considered for transfer.

At the time of fertilization check and especially after conventional IVF, it is extremely important to carefully score the cytoplasm for the presence of SER discs (see Chapter One), which are associated with the risk of a deleterious clinical outcome (Otsuki *et al.*, 2004).

Figure 201 An irregularly shaped zygote generated by ICSI showing centrally positioned PNs and a medium-sized vacuole at the 8 o'clock position in the cytoplasm (400× magnification). It was transferred but clinical outcome is unknown.

Figure 202 A zygote generated by ICSI with centrally positioned different-sized PNs, displaying two small vacuoles at the 9 o'clock position in the cytoplasm (400× magnification). It was transferred but clinical outcome is unknown.

Figure 203 A zygote generated by ICSI with an irregular oolemma and a large PVS with possibly highly fragmented polar bodies (150× magnification). Different sized overlapping PNs are peripherally positioned and several vacuoles of different sizes are present at the 2, 5 and 6 o'clock position in the cytoplasm. It was discarded.

Figure 204 A zygote generated by ICSI with slightly overlapping peripherally positioned PNs and a large PVS with one large and one fragmented polar body (150× magnification). Many small vacuoles are present throughout the cytoplasm. It was discarded.

Figure 205 Severely dysmorphic zygote generated by IVF showing small PNs and an irregularly shaped ZP and oolemma and lack of a PVS (600× magnification). There is a small vacuole present at 10 o'clock with refractile bodies immediately adjacent. It was discarded.

Figure 206 A zygote generated by ICSI showing peripherally positioned PNs and a very large vacuole at the 12 o'clock position in the cytoplasm (400× magnification). Polar bodies are fragmented and the ZP is of irregular thickness. It was discarded.

Figure 207 A zygote generated by ICSI showing cytoplasmic abnormalities (150× magnification). The PNs are juxtaposed and peripherally positioned with a large vacuole of irregular shape at the 6 o'clock position in the cytoplasm. The cytoplasm is granular and the ZP is thick and heterogeneous in appearance. It was discarded.

Figure 208 A zygote generated by ICSI showing severe cytoplasmic abnormalities (150× magnification). There is a large centralized vacuole with many small vacuoles surrounding it in a granular cytoplasm. It was discarded.

Figure 209 A zygote generated by ICSI showing peripherally located PNs with the same number and size of NPBs perfectly aligned at the PN junction (400× magnification). There is a large vacuole immediately adjacent to the two PNs that is almost the same size as the PNs. It was discarded.

Figure 210 A zygote generated by ICSI showing centrally positioned PNs and two large vacuoles immediately adjacent to each of the PNs at the 3 and 9 o'clock positions in the cytoplasm (400× magnification). There are also refractile bodies present at the 6–7 o'clock positions and an area of clustering at 11 o'clock. It was discarded.

References

Ajduk A, Ilozue T, Windsor S, Yu Y, Seres KB, Bomphrey RJ, Tom BD, Swann K, Thomas A, Graham C *et al.* Rhythmic actomyosin-driven contractions induced by sperm entry predict mammalian embryo viability. *Nat Commun* 2011;**2**:417.

Alpha Scientists in Reproductive Medicine and ESHRE Special Interest Group of Embryology. The Istanbul consensus workshop on embryo assessment: proceedings of an expert meeting. *Hum Reprod* 2011; **26**:1270–1283.

Balaban B, Urman B. Effect of oocyte morphology on embryo development and implantation. *Reprod BioMed Online* 2006; **12**:608–615.

Balaban B, Urman B, Isiklar A, Alatas C, Aksoy S, Mercan R, Mumcu A, Nuhoglu A. The effect of pronuclear morphology on embryo quality parameters and blastocyst transfer outcome. *Hum Reprod* 2001; **16**:2357–2361.

Balaban B, Yakin K, Urman b, Isiklar A, Tesarik J. Pronuclear morphology predicts embryo development and chromosome constitution. *Reprod Biomed Online* 2004;**8**:695–700.

Brezinova J, Oborna I, Svobodova M, Fingerova H. Evaluation of day one embryo quality and IVF outcome—a comparison of two scoring systems. *Reprod Biol Endocrinol* 2009;**7**:9.

Ebner T, Moser M, Sommergruber M, Gaiswinkler U, Wiesinger R, Puchner M, Tews G. Presence, but not type or degree of extension, of a cytoplasmic halo has a significant influence on preimplantation development and implantation behaviour. *Hum Reprod* 2003; **18**:2406–2412.

Ebner T, Moster M, Sommergruber M, Gaiswinkler U, Shebl O, Jesacher K, Tews G. Occurrence and developmental consequences of vacuoles throughout preimplantation development. *Fertil Steril* 2005; **83**:1635–1640.

Ebner T, Moser M, Shebl O, Sommerguber M, Tews G. Prognosis of oocytes showing aggregation of smooth endoplasmic reticulum. *Reprod Biomed Online* 2008;**16**:113–118.

Edirisinghe WR, Jemmott R, Smith C, Allan J. Association of pronuclear Z score with rates of aneuploidy in in-vitro fertilised embryos. *Reprod Fertil Dev* 2005;**17**:529–534.

Edwards RG, Beard HK. Oocyte polarity and cell determination in early mammalian embryos. *Mol Hum Reprod* 1997;**3**:863–905.

Edwards RG, Beard HK. Hypothesis: sex determination and germline formation are committed at the pronuclear stage in mammalian embryos. *Mol Hum Reprod* 1999;**5**:595–606.

Gardner RL. Can developmentally significant spatial patterning of the egg be discounted in mammals? *Hum Reprod Update* 1996;**2**:3–27.

Gardner RL. Scrambled or bissected mouse eggs and the basis of patterning in mammals. *BioEssays* 1999;**21**:271–274.

Gardner RL. Specification of embryonic axes begins before cleavage in normal mouse development. *Development* 2001;**128**:839–847.

Garello C, Baker H, Rai J, Montgomery S, Wilson P, Kennedy CR, Hartshorne GM. Pronuclear orientation, polar body placement, and embryo quality after intracytoplasmic sperm injection and in vitro fertilization: further evidence for polarity in human oocytes? *Hum Reprod* 1999;**14**:2588–2595.

Gianaroli L, Magli MC, Ferraretti AP, Fortini D, Grieco N. Pronuclear morphology and chromosomal abnormalities as scoring criteria for embryo selection. *Fertil Steril* 2003;**80**:341–349.

James AN, Hennessy S, Reggio B, Wiemer K, Larsen F, Cohen J. The limited importance of pronuclear scoring of human zygotes. *Hum Reprod* 2006;**21**:1599–1604.

Kahraman S, Yakin K, Dönmez E, Samli H, Bahçe M, Cengiz G, Sertyel S, Samli M, Imirzalioğlu N. Relationship between granular cytoplasm of oocytes and pregnancy outcome following intracytoplasmic sperm injection. *Hum Reprod* 2000;**15**:2390–2393.

Lundin K, Bergh C, Hardarson T. Early embryo cleavage is a strong indicator of embryo quality in human IVF. *Hum Reprod* 2001; **16**:2652–2657.

Meriano JS, Alexis J, Visram-Zaver S, Cruz M, Casper RF. Tracking of oocyte dysmorphisms for ICSI patients may prove relevant to the outcome in subsequent patient cycles. *Hum Reprod* 2001; **16**:2118–2123.

Montag M, van der Ven H. Evaluation of pronuclear morphology as the only selection criterion for further embryo culture and transfer: results of a prospective multicentre study. *Hum Reprod* 2001; **16**:2384–2389.

Montag M, Liebenthron J, Köster M. Which morphological scoring system is relevant in human embryo development? *Placenta* 2011; **32**:S252–S256.

Munné S, Cohen J. Chromosome abnormalities in human embryos. *Hum Reprod Update* 1998;**4**:842–855.

Nagy ZP, Janssenswillen C, Janssens R, De Vos A, Staessen C, Van deVelde H, Van Steirteghem AC. Timing of oocyte activation, pronucleus formation and cleavage in humans after intracytoplasmic sperm injection (ICSI) with testicular spermatozoa and after ICSI or in-vitro fertilization on sibling oocytes with ejaculated spermatozoa. *Hum Reprod* 1998;**13**:1606–1612.

Nagy ZP, Dozortsev D, Diamond M, Rienzi L, Ubaldi F, Abdelmassih R, Greco E. Pronuclear morphology evaluation with subsequent evaluation of embryo morphology significantly increases implantation rates. *Fertil Steril* 2003;**80**:67–74.

Nicoli A, Valli B, Di Girolamo R, Di Tommaso B, Gallinelli A, La Sala GB. Limited importance of pre-embryo pronuclear morphology (zygote score) in assisted reproduction outcome in the absence of embryo cryopreservation. *Fertil Steril* 2007;**88**:1167–1173.

Nicoli A, Capodanno F, Moscato L, Rondini I, Villani MT, Tuzio A, La Sala GB. Analysis of pronuclear zygote configurations in 459 clinical pregnancies obtained with assisted reproductive technique procedures. *Reprod Biol Endocrinol* 2010;**8**:77.

Otsuki J, Okada A, Morimoto K, Nagai Y, Kubo H. The relationship between pregnancy outcome and smooth endoplasmic reticulum clusters in MII human oocytes. *Hum Reprod* 2004;**19**:1591–1597.

Palermo G, Munné S, Cohen J. The human zygote inherits its mitotic potential from the male gamete. *Fertil Steril* 1994;**9**:1220–1225.

Payne D, Flaherty SP, Barry MF, Matthews CD. Preliminary observations on polar body extrusion and pronuclear formation in human oocytes using time-lapse video cinematography. *Hum Reprod* 1997;**12**:532–541.

Payne JF, Raburn DJ, Couchman GM, Price TM, Jamison MG, Walmer DK. Relationship between pre-embryo pronuclear morphology (zygote score) and standard day 2 or 3 embryo morphology with regard to assisted reproductive technique outcomes. *Fertil Steril* 2005; **84**:900–909.

Pedersen T. Growth factors in the nucleolus? *J Cell Biol* 1998; **143**:279–281.

Plachot M. Fertilization. *Hum Reprod* 2000;**15**(Suppl. 4):19–30.

Reichman DE, Jackson KV, Racowscky C. Incidence and development of zygotes exhibiting abnormal pronuclear disposition after identification of two pronuclei at the fertilization check. *Fertil Steril* 2010;**94**:965–970.

Sadowy S, Tomkin G, Munné S, Ferrara-Congedo T, Cohen J. Impaired development of zygotes with uneven pronuclear size. *Zygote* 1998; **6**:137–141.

Sakkas D, Shoukir Y, Chardonnens D, Bianchi PG, Campana A. Early cleavage of human embryos to the two-cell stage after intracytoplasmic sperm injection as an indicator of embryo viability. *Hum Reprod* 1998;**13**:182–187.

Sathananthan AH, Ratnam SS, Ng SC, Tarin JJ, Gianaroli L, Trounson A. The sperm centriole: its inheritance, replication and perpetuation in early embryos. *Hum Reprod* 1996;**11**:345–356.

Scott L. Oocyte and embryo polarity. *Semin Reprod Med* 2001; **18**:171–183.

Scott L. Pronuclear scoring as a predictor of embryo development. *Reprod Biomed Online* 2003;**6**:201–214.

Scott LA, Smith S. The successful use of pronuclear embryo transfers the day following oocyte retrieval. *Hum Reprod* 1998;**13**: 1003–1013.

Scott L, Alvero R, Leondires M, Miller B. The morphology of human pronuclear embryos is positively related to blastocyst development and implantation. *Hum Reprod* 2000;**15**:2394–2403.

Scott L, Finn A, O'Leary T, McLellan S, Hill J. Morphologic parameters of early cleavage-stage embryos that correlate with fetal development and delivery: prospective and applied data for increased pregnancy rates. *Hum Reprod* 2007;**22**:230–240.

Senn A, Urner F, Chanson A, Primi MP, Wirthner DW, Germond M. Morphological scoring of human pronuclear zygotes for prediction of pregnancy outcome. *Hum Reprod* 2006;**21**:234–239.

Svarcova O, Dinnyes A, Polgar Z, Bodo S, Adorjan M, Meng Q, Maddox-Hyttel P. Nucleolar re-activation is delayed in mouse embryos cloned from two different cell lines. *Mol Reprod Dev* 2009; **76**:132–141.

Tesarik J, Greco E. The probability of abnormal preimplantation development can be predicted by a single static observation on pronuclear stage morphology. *Hum Reprod* 1999;**14**:1318–1323.

Tesarik J, Junca AM, Hazout A, Aubriot FX, Nathan C, Cohen-Bacrie P, Dumont-Hassan M. Embryos and high implantation potential after intracytoplasmic sperm injection can be recognized by a simple, non-invasive examination of pronuclear morphology. *Hum Reprod* 2000; **15**:1396–1399.

Van Blerkom J, Henry G. Oocyte dysmorphism and aneuploidy in meiotically mature human oocytes after ovarian stimulation. *Hum Reprod* 1992;**7**:379–390.

Van Blerkom J, Davis P, Merriam J, Sinclair J. Nuclear and cytoplasmic dynamics of sperm penetration, pronuclear formation and micro-tubule organization during fertilization and early preimplantation development in the human. *Hum Reprod Update* 1995;**1**:429–461.

Van Blerkom J, Antczak M, Schrader R. The developmental potential of the human oocyte is related to the dissolved oxygen content of follicular fluid: association with vascular endothelial growth factor levels and perifollicular blood flow characteristics. *Hum Reprod* 1997; **12**:1047–1055.

Weitzman VN, Schnee-Riesz J, Benadiva C, Nulsen J, Siano L, Maier D. Predictive value of embryo grading for embryos with known outcomes. *Fertil Steril* 2010;**93**:658–662.

Yan J, Li Y, Shi Y, Feng HL, Gao S, Chenz Z. Assessment of sex chromosomes of human embryos arising from monopronucleus zygotes in in vitro fertilization and intracytoplasmic sperm injection cycles of Chinese women. *Gynecol Obstet Invest* 2010;**69**:20–23.

Zamora RB, Sánchez RV, Pérez JG, Diaz RR, Quintana DB, Bethencourt JC. Human zygote morphological indicators of high rate of arrest at the first cleavage stage. *Zygote* 2011;**19**:339–344.

Zollner U, Zollner KP, Steck T, Dietl J. Pronuclear scoring: time for international standardization. *J Reprod Med* 2003;**5**:365–369.